Research Square

Preprints are preliminary reports that have not undergone peer review.
They should not be considered conclusive, used to inform clinical practice,
or referenced by the media as validated information.

Evaluation of Real Time Magnetic Resonance Imaging and Keypoint Detection Models for Assessing Range of Motion in Ankle Braces: A Study on Healthy Individuals

Jonathan van Dieken

jonathan.vandieken@med.uni-goettingen.de

Universitätsmedizin Göttingen

Benedikt Kieslich

Universitätsmedizin Göttingen

Günther Engel

Universitätsmedizin Göttingen

Fabian Kück

Universitätsmedizin Göttingen

Hazibullah Waizy

Orthoprofis

Sebastian Aeffner

Universitätsmedizin Göttingen

Simon Friedrich Rösel

Universitätsmedizin Göttingen

Ali Seif Amir Hosseini

Universitätsmedizin Göttingen

Arndt F. Schilling

Universitätsmedizin Göttingen

Babak Panahi

Universitätsmedizin Göttingen

Research Article

Keywords: real time imaging, real time MRI, dynamic imaging, ankle instability, ankle brace

Posted Date: March 11th, 2026

DOI: https://doi.org/10.21203/rs.3.rs-8719220/v1

License: This work is licensed under a Creative Commons Attribution 4.0 International License.
Read Full License

Additional Declarations: No competing interests reported.

Abstract

Introduction**:** Acute ankle sprains are prevalent injuries in physically active individuals. Functional support through the use of braces is a common approach to prevent excessive movements and reinjury to the affected ligaments.

Recent advancements in imaging technology, particularly real-time magnetic resonance imaging (rtMRI), present new opportunities for evaluating physiological movements. This study aims to investigate the applicability of rtMRI in measuring the range of motion (ROM) of the talocrural joint while utilizing four different types of ankle braces.

Methods: 45 dynamic rtMRI exams were performed in a cohort of 9 participants at the University Medical Center Göttingen with and without four commercially available brace models during plantar flexion, dorsiflexion, eversion and inversion.

Two observers measured the angles between predefined anatomical keypoints at intervals of every ten images. In addition, a keypoint detection model (YOLO11) was trained and utilized as a third observer.

Intraclass Correlation Coefficients (ICC) and the relative mobility restriction for each brace model were calculated. T-tests and linear mixed models were used for the analysis of differences between the brace models and observers.

Results: All ankle braces significantly reduced the range of motion (ROM) in the sagittal plane by up to 38% compared to unrestricted movement. Sagittal measurements demonstrated a high level of interobserver agreement between two human observers and the keypoint detection model, with a consistency Intraclass Correlation Coefficient (ICC) of 0.92. This agreement was even higher in a subset of studies that adhered to predefined image quality standards, yielding a consistency ICC of 0.96. Coronal measurements showed low interobserver agreement presumably due to suboptimal image quality resulting from unwanted rotational movements, which influenced the visibility of the predefined anatomical landmarks.

Conclusion: These findings suggests that rtMRI has the potential for accurate measurement of talocrural joint ROM in the context of evaluating ankle braces. However, imaging studies have to meet quality criteria to ensure high interobserver reliability. Furthermore, the implementation of keypoint detection algorithms can facilitate automated angle measurements, streamlining a time-consuming process for radiologists.

Trial Registration:

The study was retrospectively registered in the DRKS database on April 1st, 2025 with the identifier DRKS00036544.

Background

Acute ankle sprain represents the most prevalent musculoskeletal injury, accounting for up to 30% of all sports-related injuries (1). The most common form of ankle sprain involves the stretching or tearing of the lateral ankle ligament complex (2). Functional support through the use of ankle braces has been extensively researched and is recommended for a duration of 4–6 weeks by several authors, surpassing alternatives such as kinesiotaping or immobilization (1, 3). There is a variety of different brace designs by several manufacturers (4). Ankle braces are designed to provide mechanical stability, proprioception and psychological confidence (5). A systematic review by Megalaa et al. found that ankle braces did not significantly reduce ankle inversion (6). In contrast, Rowe et al. concluded that while frontal plane movements were not notably affected during running, there was minimal evidence suggesting restriction during landing; however, movements in the sagittal plane were significantly reduced (5).

Acute ankle sprain can lead to long-term posttraumatic problems in up to 70% of cases, including posttraumatic osteoarthritis and chronic ankle instability, which is itself associated with impaired postural control (7, 8). Ankle brace treatment has proven effective in reducing the risk of reinjury (9). Beyond this primary indication, ankle braces are utilized for a variety of conditions, ranging from inflammation of the joint capsule or tendons to stable fractures of the lateral malleolus (10, 11).

Real time magnetic resonance imaging (rtMRI) is an emerging technique capable of visualizing motion with a temporal resolution of up to 20 ms (12). The technique was first introduced by Uecker et al. in 2010 building upon fast low-angle shot acquisitions and undersampled radially acquired k-space data (12). This approach allows for highly efficient k-space sampling, with each so called “spoke” traversing through the k-space center. Iterative reconstruction techniques further reduce the number of spokes required (13).

Recent studies have demonstrated the feasibility of using rtMRI to visualize the scapholunate joint during wrist motion, potentially aiding in the diagnosis of carpal instability by enabling precise measurement of scapholunate joint width (14, 15).

A study by Sheehan et al. demonstrated that the talocrural joint plays an important role in ankle kinematics, even during supination which is usually attributed to the subtalar joint (16).

The goal of this study was to leverage rtMRI to visualize talocrural joint motion in the sagittal and frontal planes, examining the mobility restriction induced by different types of ankle braces. In this radiation-free approach we compared the range of motion across four distinct brace designs from various manufacturers against physiological, unrestricted movement.

Methods

Study design and Participants

This study was performed at the University Medical Center Göttingen, Germany, following the approval of the ethics committee (protocol code 15/3/18). A total of ten healthy participants were recruited based on specific inclusion and exclusion criteria. Written informed consent was obtained from each participant.

Qualified participants had no history of surgical intervention related to the ankle or prior ankle injuries. Individuals with known ligamentous diseases or rheumatologic conditions were excluded from the study, as were those with chronic health issues such as arterial hypertension or diabetes. Additional exclusion criteria included a bodyweight exceeding 125 kg and a waist circumference that exceeded the bore size of our MRI machine, which was 70 cm in diameter. Individuals with contraindications for MRI examination were also excluded. To ensure optimal imaging conditions, all participants were instructed to refrain from engaging in any physical activities that could strain the ankle for 48 hours prior to the examination.

Image acquisition

Participants were positioned in the MRI scanner (3T Skyra, Siemens Healthineers, Erlangen, Germany) in a supine position, feet-first. A 16-channel multipurpose coil (Variety, Noras MRI products GmbH, Höchberg, Germany) was then placed around the ankle. The ankle was then placed in a specifically designed apparatus that simulated passive inversion and eversion movements (Fig. 1).

Figure 1: Computer Aided Design (1) *and schematic drawing* (2) *of the specifically designed apparatus for the simulation of eversion and eversion of the ankle joint and MRI setup* (3) *for measuring the range of motion in inversion and eversion. Written consent was obtained regarding the publication of these images.*

The imaging protocol comprised both static and dynamic sequences, resulting in a total acquisition time of approximately 90 minutes.

Initially, static T1-weighted Turbo Spin-Echo and T2-weigthed Double-Echo Steady State sequences were acquired in the sagittal plane to identify any occult ankle pathology. Localizer images were acquired to plan the dynamic sequences.

Dynamic imaging utilized T1-weighted rtMRI sequences based on a RF-spoiled fast low-angle short (FLASH) gradient-echo technique (TR = 2.94 ms (sagittal) / 3.08 ms (coronal), TE = 1.79 ms (sagittal)/ 1.85 ms (coronal), flip angle 8°). This technique was enhanced by a radial encoding scheme and iterative reconstruction using regularized nonlinear inversion (NLINV).

Initially, passive frontal-plane movements were performed using the above-mentioned apparatus, resulting in the acquisition of a total of 300 images at a temporal resolution of 20 ms. The imaging parameters included a field of view of 128 mm and a matrix of 128 x 128, yielding an in-plane resolution of 1.0 mm. The slice thickness was set at 4 mm (Table 1).

Following this phase, the apparatus was removed, and participants were instructed to perform dorsiflexion and plantar flexion through their full range of motion while sagittal images were acquired.

Table 1
Acquisition parameters of coronal and sagittal rtMRI sequences.

	Sagittal	Coronal
Image count	400	300
Slice Thickness (mm)	4	4
Field-of-view (mm)	128	127
Resolution (Pixel)	128	128
Flip Angle	8°	8°
TE (ms)	1.79	1.85
TR (ms)	2.94	3.08
Temporal resolution (ms)	20	20

Following the assessment of the physiological range of motion, four different ankle braces were sequentially applied around each participant's ankle. The dynamic imaging sequence was then repeated for each brace model. To mitigate potential fatigue effects, the order of brace application was randomized among participants.

The NLINV-reconstruction of real time images was performed by using a reconstruction computer (sysGen/TYAN Octuple-GPU, Sysgen; equipped with 8 Nvidia GeForce GTX TITAN GPUs), which was fully integrated into the commercial MRI system.

The acquired MRI data were post-processed using the MATLAB software package (MathWorks R2024a, Inc., Natick, Massachusetts, USA).

Ankle Brace types:

In this study, one flexible and three semi-rigid ankle braces, which were commonly utilized in clinical practice, were selected for evaluation (Fig. 2):

Push Med Ankle Brace (Ofa Bamberg GmbH, Bamberg, Germany):

The Push Med ankle brace is a flexible support device made from microfiber and featuring elastic straps to allow individual adaptation and compression. The brace also includes a silicon plate on the inside to enhance proprioception. According to the manufacturer, this product limits both ankle eversion and inversion.

Aircast Air-Stirrup II (DJO France, S.A.S., Mouguerre, France):

The Aircast Air-Stirrup II is a semi-rigid ankle brace featuring a stirrup design. It contains air chambers on the inside, which are compressed during walking. As the user walks, the contained air is displaced from the plantar chamber to the lateral chambers, creating a massaging compression effect from distal to proximal. This mechanism is intended to support pain relief and reduce joint swelling.

Malleo TriStep 50S8N (Ottobock SE & Co. KgaA, Otto Bock Health Care GmbH, Duderstadt, Germany):

The Malleo TriStep is a semi-rigid ankle brace with a three-part construction that allows progressive adaptation throughout the healing process. During the initial phase of the recovery the brace is worn in combination with a rigid foot plate and a cross belt. As the healing progresses, the foot plate can be removed for a more flexible configuration. In the final phase, only the brace itself is worn, allowing increased mobility.

Juzo Pro Malleo Light (Julius Zorn GmbH, Aichach, Germany):

The Juzo Pro Malleo Light's features a semi-rigid stirrup design that allows for individualized adjustment through multiple straps and a heel band. According to the manufacturer, this design effectively limits both eversion and inversion of the ankle, potentially reducing the risk of reinjury during physical activities.

Measurements:

Image quality for all sagittal sequences was assessed using a five-point Likert scale (Supplemental Table 1) by three radiologists with varying levels of experience (3, 8 and 15 years). In both coronal and sagittal sequences, angles were measured every ten images between the articulating bones of the talocrural joint. To ensure reproducibility, anatomical landmarks were clearly defined prior to measurement. In the sagittal plane, the angle was defined as the intersection between a line connecting the distal ventral and dorsal edges of the tibia and a line between the posterior processus of the calcaneus and the dorsal edge of the talar head. In the coronal plane angles were determined between a line connecting the distal tips of the malleoli and the surface of the trochlea tali (Fig. 3). All measurements were performed by two observers, with 1 and 3 years of experience in musculoskeletal radiology, utilizing the Horos Software (version 3.3.6, LGPL-3.0)(17, 18).

Deep-learning model:

An openly available deep-learning keypoint detection model (YOLO11, Ultralytics Inc.) was trained for automated keypoint detection and angle measurements, as described before (19). The image series that were acquired without the use of an ankle brace and an average Likert-score of greater than 3 were selected for the training of the model. A total of 300 images were randomly selected sparing every tenth image and manually annotated by a radiologist with three years of experience. Training was performed in a Google Colab environment for 300 epochs, following extensive hyperparameter tuning using the

software's built-in optimization method. Subsequently, all acquired sequences were measured automatically in prediction mode, again considering every tenth image.

Statistics:

For each ankle brace, as well as the physiological joint, we calculated the range of motion (ROM) represented by the difference of the angles measured at minimum and maximum inversion and eversion. The mean, standard deviation, maximum and minimum values were calculated.

Relative mobility restriction rD was determined as the difference between the ROM with and without an ankle brace divided by the unrestricted ROM:

$$r\Delta = \frac{(maxAngle_{withoutAB} - minAngle_{withoutAB}) - (maxAngle_{withAB} - minAngle_{withAB})}{(maxAngle_{withoutAB} - minAngle_{withoutAB})}$$

A two-tailed one-sample Student's t-test was applied to the relative mobility restriction rD for each brace model and direction of movement to test against the null hypothesis of no constraint.

For the interobserver analysis, linear mixed models with observer (including both human observers and, for the measurements in the sagittal images, the pose-detection model) and brace model (including no brace) as fixed effects and a random intercept for the individual were employed to assess systematic differences between the observers. Estimated mean differences of the measured angles in the sagittal and the coronal images, respectively, between the observers were reported. These differences were accompanied by 95% confidence intervals and p values. Additionally, consistency intraclass correlation coefficients (ICC) were computed to evaluate interobserver consistency in angle measurements. This was performed separately for both the sagittal and the coronal images.

A sub-analysis was performed on sagittal images that achieved an average Likert score of 3 or higher.

Statistical analysis was performed using the R software (Version 4.2.3; R Core Team 2023) with the R-packages lme4 (version 1.1.35.5) and lmerTest (version 3.1.3) for linear mixed models and performance (version 0.12.4) for the computation of ICCs. The significance threshold was established at 5%. P-values of the t-tests were adjusted using the Bonferroni-correction to account for multiple comparisons.

Results

Nine participants completed the entire examination; however, one participant was excluded due to an unphysiologically low range of motion during dorsiflexion resulting in a total of 8 participants and 40 individual scans for the final analysis. The average height of the participants was 173 cm (SD ± 9.3), average weight was 64 kg (SD ± 9.4) and the average BMI was 21 kg/m² (SD ± 1.4).

Examination of the unbraced ankle showed a minimal angle of -14.0° (SD ± 8.0) and a maximum angle of 37.0° (SD ± 7.0) in the sagittal plane, resulting in a total range of motion of 51° (SD ± 12.0). When wearing the Juzo Pro Malleo, an average ROM of 41.0° (SD ± 13.0) was observed, whereas an average ROM of

40.0° (SD ± 12.0) was determined for the Push med ankle brace and a ROM of 37.0° (SD ± 9.0) for the Aircast Air-Stirrup II. The MalleoTriStep demonstrated an average ROM of 31.0° (SD ± 9.0). The relative mobility restriction in the sagittal plane was highest for the MalleoTriStep at 0.38 (SD ± 0.13, $p < 0.001$), followed by the Aircast Air-Stirrup II at 0.27 (SD ± 0.09, $p < 0.001$), the Push med ankle brace at 0.23 (SD ± 0.16, $p = 0.017$), and the Juzo Pro Malleo at 0.2 (SD ± 0.1, $p = 0.002$) (Fig. 4).

During passive inversion and eversion in the coronal plane, an average maximum angle of 19.0° (SD ± 4.0) was measured, alongside a minimum angle of 12.0° (SD ± 4.0) resulting in an average ROM of 7.1° (SD ± 2.5). The average ROM for the Juzo Pro Malleo was 6.5° (SD ± 3.4), while 5.6° (SD ± 1.4) for the Push med ankle brace, 5.5° (SD ± 1.7) for the Aircast Air-Stirrup II and 5.7° (SD ± 2.4) for the Malleo TriStep. The relative mobility restriction in the coronal plane was 0.05 (SD ± 0.37, $p = 1.0$) for the Juzo Pro Malleo, 0.16 (SD ± 0.28, $p = 1.0$) for the Push med ankle brace, 0.11 (SD ± 0.47, $p = 1.0$) for the Aircast Air-Stirrup II and 0.1 (SD ± 0.47, $p = 1.0$) for the Malleo TriStep (Fig. 5).

Interobserver analysis was conducted independently for both coronal and sagittal measurements. The analysis of sagittal measurements revealed significant differences between all three observers. Specifically, Observer 1 and 2 exhibited an estimated mean difference by 1.47° (CI [0.4, 2.54], $p = 0.004$) across all sagittal measurements. The estimated mean difference between the keypoint detection model and observer 1 was − 0.27° (CI [-1.34, 0.79], $p = 0.819$), indicating no significant discrepancy. In contrast, Observer 2 and the keypoint detection model showed an estimated mean difference of -1.75° (CI [-2.82, -0.68], $p < 0.001$). Consistency ICCs for all observers were 0.92 and 0.97 between the human observers.

Interobserver analysis of coronal measurements showed an estimated mean difference of 0.32° (CI [0.17, 0.47]) between the two human observers ($p < 0.001$), with a consistency ICC of 0.49.

A sub-analysis of 39 out of 45 sagittal image series with an average Likert score of 3 or more showed an estimated mean difference of -0.33° (CI [-1.2, 0.55], $p = 0.74$) between Observer 1 and the keypoint detection model. Observer 1 and 2 differed by 1.51° (CI [0.46, 2.56], $p = 0.002$) and Observer 2 and the keypoint detection model by -1.84° (CI [-2.89, -0.79], $p < 0.001$). The consistency ICC was 0.96 for all three observers, 0.98 for Observer 1 and 2, and 0.95 and 0.94 for keypoint detection model and Observers 1 and 2, respectively.

Discussion

This study demonstrates that both active and passive ankle movements can be imaged with high temporal resolution using real-time magnetic resonance imaging (rtMRI). To our knowledge, this is the first study to utilize this new technique for visualizing motion in the talocrural joint. However, generalizability is very limited owing to the small sample size in this study. Thus, it should rather be viewed as a proof-of-concept.

All four ankle braces significantly restricted both dorsiflexion and plantar flexion, with the MalleoTriStep brace exhibiting the greatest degree of mobility restriction at 38% compared to the unbraced ankle

reducing the ROM from 51° to 31°. Nevertheless, it is worth mentioning that the performed movements may not fully represent real-world functional activities.

Contrary to our expectations, inversion and eversion in the talocrural joint were not significantly reduced by any of the tested braces. These findings align with the results reported by Megalaa et al. (6), who performed a review of 42 studies investigating mobility restriction through ankle braces and taping, primarily in healthy individuals. In our study, we exclusively measured the range of motion of the talocrural joint in the coronal plane, as the ligaments stabilizing the talocrural joint - particularly the anterior talocalcaneal ligament - are susceptible to injury from lateral ankle sprain (20). In addition, biomechanical studies have shown that the talocrural joint contributes significantly to eversion and inversion movements (16). The review indicated that while ankle braces did not decrease range of motion in the coronal plane, they did reduced range of motion in the sagittal plane, particularly during plantar flexion. As the effectiveness of ankle braces in preventing ankle sprains has been demonstrated in several studies, the protective effect is likely due to prevention of movements exceeding the physiological range of motion.

On the other hand, we measured a significant mobility restriction in the sagittal plane, which aligns with the results of the above-mentioned meta-analysis. The anatomical configuration of the talus body, which narrows slightly towards the dorsal aspect, resulting in increased ankle mobility in plantar flexion (21). The braces' ability to reduce plantar flexion may serve as an additional mechanism for providing stability and preventing excessive motion. In addition, plantar flexion > 20° has been shown to increase tensile stress on the anterior talofibular ligament. Bracing may therefore prevent healing in elongation, which can result in chronic instability (22).

Finally, further studies regarding mobility restriction in the injured ankle will be necessary. However, applying potentially excessive movement to an already injured ankle can interfere with the healing process and retraumatize the involved ligaments. Therefore, the ethical implications of such study design must be carefully considered, as they may lead to chronic instability and long-term disability.

The interobserver analysis revealed significant differences in angle measurements between observer 1 and 2, as well as between observer 2 and the pose detection model, specifically regarding sagittal movement. The estimated mean angles differed by 1.47° and − 1.75° respectively. Given the large number of images analyzed in this study, even minor discrepancies between two observers can be detected with high statistical power. However, considering that the tibiotalar joint's range of motion exceeds 50° in the sagittal plane, these differences appear relatively small. The large consistency intraclass correlation coefficient indicates high consistency between observers when disregarding systematic differences.

In contrast, coronal measurements showed a low consistency intraclass correlation, whereas the estimated mean difference between Observers 1 and 2 was minimal (0.32°). The inability to strictly confine eversion and inversion in the talocrural joint to the acquisition plane was due to slight rotational movements, which resulted in non-visibility of the malleolar tips.

An additional sub-analysis of sagittal scans with an at least adequate image quality showed that interobserver variability could be reduced even further, if certain quality criteria were fulfilled. However, the

absolute differences in angle measurements between the observers and the keypoint detection model stayed similar.

In conclusion, the ROM measured on rt-MRI demonstrates high reproducibility, provided that acceptable image quality is achieved. This radiation-free approach holds significant potential for advancing the development of ankle braces, as it facilitates the evaluation of brace effectiveness in a dynamic setting. Additionally, rt-MRI may represent a key technique towards designing customized braces to serve individual purposes (23, 24). To guide future examinations, we propose a set of quality criteria that should be adhered to, or at least considered, to ensure reproducible and reliable measurements. These criteria include the visibility of keypoints, contrast, spatial and temporal resolution, the field of view, and appropriate patient selection and positioning (Table 2).

Table 2
Proposed quality criteria for rtMRI of the joint.

Category	Considerations
Anatomical Keypoint Visibility	• Key anatomical structures are clearly visible. • No structures are obscured due to artifacts or malpositioning. This may e.g. include choosing metal (and artifact) free products for brace testing.
Contrast	• Image contrast allows for clear differentiation of tissues or structures. • Signal-to-noise ratio (SNR) is adequate to maintain diagnostic utility.
Spatial resolution	• Adequate resolution for the targeted anatomy.
Temporal resolution	• Sufficient temporal resolution to capture real-time physiological motion. • No excessive trade-offs between spatial and temporal resolution.
Field of View	• FOV appropriately covers the region of interest. • FOV covers the entire region during the full range of motion
Patient Positioning and Selection	• If possible, the examined movement should be limited to the plane of image acquisition to prevent unintentional out-of-plane movements • No metal hardware in or close to the examined joint

In our opinion, these criteria represent the ideal conditions for real-time imaging; however, previous studies have shown that confining movement to the acquisition plane is not always feasible. For instance, rtMRI of the scapholunate joint is limited by palmar inclination of the scaphoid during radial deviation of the wrist (15). Future approaches may benefit from the parallel acquisition of several slices simultaneously, which could enable determination of the rotation angle of the involved bones through the application of a fitting algorithm.

Finally, this study has shown that a deep-learning based keypoint detection algorithm can effectively compute tibiotalar angles during rtMRI acquisitions. However, individual measurements may differ from

those performed by a human reader due to misidentification of the keypoints. When assessing ROM, this issue does not significantly impact the overall results, as all automated measurements are likely to be affected by the same degree of error. Furthermore, the agreement between human readers and the keypoint detection algorithm was strongest when the acquisitions met at least image quality standards, defined as a Likert-Score of 3 or higher.

A potential limitation of this of this study is the scarce availability of truly independent training data. We ensured not to use the same images for training and evaluation, but due to a high temporal resolution sequential images differed only minimally. In future studies, the algorithm should be validated on an independent cohort.

Over the past decades, the approach to postoperative and posttraumatic treatment has shifted from immobilization to early mobilization (25). rtMRI could serve as a valuable tool for dynamic imaging of the affected joint structures, helping to identify instabilities that may lead to poor treatment outcomes. Additionally, rtMRI has potential applications for other joints, such as detecting glenohumeral instability or visualizing joint kinematics after ACL surgery, to name a few. This study highlights the potential of rtMRI as a robust tool for assessing ankle mobility and brace effectiveness with high accuracy. By integrating deep-learning-based keypoint detection, we pave the way for more efficient, automated analyses, reducing the workload for radiologists. With further improvements, this technology could revolutionize orthopedic diagnostics and rehabilitation as well as brace development, enhancing patient care.

Abbreviations

AB
ankle brace
CI
confidence intervall
FOV
field of view
ICC
intraclass correlation coefficient
NLINV
nonlinear inversion
rΔ
relative mobility restriction
ROM
range of motion
rtMRI
real-time magnetic resonance imaging
SD
standard deviation

SNR
signal-to-noise ratio

Declarations

Ethics approval and consent to participate:

This study was approved by the local ethics committee (University Medical Center Göttingen, Germany, protocol code 15/3/18) and was conducted in accordance with the Declaration of Helsinki. Written informed consent was obtained from all participants of this study.

Consent for publication:

Written informed consent regarding the publication of personal data was obtained from all individuals, whose images (Figures 1 and 2) were used in this manuscript.

Availability of data and materials:

The datasets generated and/or analysed during the current study are not publicly available due to privacy or ethical restrictions but are available from the corresponding author on reasonable request.

Competing interests:

The authors declare that they have no competing interests.

Funding:

This project did not receive specific funding and was conducted as part of the employment of the authors at the University Medical Center Göttingen, Germany.

Authors' contribution:

Conceptualization and Methodology: BP, ASAH and HW; Data Curation: BP, JE and BK; Formal Analysis: FK; Investigation: JE and BK; Project Administration: BP and AFS; Resources: BP and ASAH Supervision: ASAH; Visualization: JE and BK; Writing – original draft: JE and BK; Writing – editing and review: SFR, SA, BP and GE The final manuscript was read and approved by all authors.

Acknowledgements:

- Robin Wilke kindly provided the apparatus for passive inversion and eversion used in this project as well as the Computer Aided Design and schematic drawing shown in Figure 1.
- As indicated in the "Materials and Methods" section, YOLO11 (Ultralytics) was used in this study.

References

1. Kemler E, van de Port I, Backx F, van Dijk CN. A Systematic Review on the Treatment of Acute Ankle Sprain. Sports Medicine. 2011 Mar;41(3):185–97.
2. Herzog MM, Kerr ZY, Marshall SW, Wikstrom EA. Epidemiology of Ankle Sprains and Chronic Ankle Instability. J Athl Train. 2019 Jun 1;54(6):603–10.
3. Ruiz-Sánchez FJ, Ruiz-Muñoz M, Martín-Martín J, Coheña-Jimenez M, Perez-Belloso AJ, Pilar Romero-Galisteo R, et al. Management and treatment of ankle sprain according to clinical practice guidelines: A PRISMA systematic review. Medicine. 2022 Oct 21;101(42):e31087.
4. Sprouse RA, McLaughlin AM, Harris GD. Braces and Splints for Common Musculoskeletal Conditions. Am Fam Physician. 2018 Nov 15;98(10):570–6.
5. Rowe PL, Bryant AL, Egerton T, Paterson KL. External Ankle Support and Ankle Biomechanics in Chronic Ankle Instability: Systematic Review and Meta-Analysis. J Athl Train. 2023 Jul 1;58(7–8):635–47.
6. Megalaa T, Hiller CE, Ferreira GE, Beckenkamp PR, Pappas E. The effect of ankle supports on lower limb biomechanics during functional tasks: A systematic review with meta-analysis. J Sci Med Sport. 2022 Jul;25(7):615–30.
7. Gribble PA, Bleakley CM, Caulfield BM, Docherty CL, Fourchet F, Fong DTP, et al. Evidence review for the 2016 International Ankle Consortium consensus statement on the prevalence, impact and long-term consequences of lateral ankle sprains. Br J Sports Med. 2016 Dec;50(24):1496–505.
8. Majlesi M. Identifying the Most Sensitive COP Variable in Static Balance: The Impact of Chronic Ankle Instability on Postural Stability. J Foot Ankle Res. 2025 Sep;18(3).
9. Surve I, Schwellnus MP, Noakes T, Lombard C. A Fivefold Reduction in the Incidence of Recurrent Ankle Sprains in Soccer Players Using the Sport-Stirrup Orthosis. Am J Sports Med. 1994 Sep 23;22(5):601–6.
10. Drakos MC, Murphy CI. Bracing Versus Casting in Ankle Fractures. Phys Sportsmed. 2014 Nov 13;42(4):60–70.
11. Le V, Veljkovic A, Salat P, Wing K, Penner M, Younger A. Ankle Arthritis. Foot Ankle Orthop. 2019 Jul 1;4(3).
12. Uecker M, Zhang S, Voit D, Karaus A, Merboldt K, Frahm J. Real-time MRI at a resolution of 20 ms. NMR Biomed. 2010 Oct 27;23(8):986–94.
13. Uecker M, Zhang S, Frahm J. Nonlinear inverse reconstruction for real-time MRI of the human heart using undersampled radial FLASH. Magn Reson Med. 2010 Jun 21;63(6):1456–62.
14. Shaw CB, Foster BH, Borgese M, Boutin RD, Bateni C, Boonsri P, et al. Real-time three-dimensional MRI for the assessment of dynamic carpal instability. PLoS One. 2019 Sep 19;14(9):e0222704.
15. Ehmig J, Lehmann K, Engel G, Kück F, Lotz J, Aeffner S, et al. Measurement of Scapholunate Joint Space Width on Real-Time MRI—A Feasibility Study. Diagnostics. 2024 Jun 3;14(11):1177.
16. Sheehan FT, Seisler AR, Siegel KL. In Vivo Talocrural and Subtalar Kinematics: A Non-invasive 3D Dynamic MRI Study. Foot Ankle Int. 2007 Mar 1;28(3):323–35.
17. Horos. Annapolis, MD, USA: Nimble Co LLC d/b/a Purview; 2024.

18. R Core Team. R: A Language and Environment for Statistical Computing. Vienna, Austria: R Foundation for Statistical Computing; 2018.
19. Jocher G, Qiu J. Ultralytics YOLO11. 2024.
20. Medina McKeon JM, Hoch MC. The Ankle-Joint Complex: A Kinesiologic Approach to Lateral Ankle Sprains. J Athl Train. 2019 Jun 1;54(6):589–602.
21. Brockett CL, Chapman GJ. Biomechanics of the ankle. Orthop Trauma. 2016 Jun;30(3):232–8.
22. Waizy H, Harrasser N, Fehske K. Außenbandverletzungen. Unfallchirurg. 2018 Sep 27;121(9):683–92.
23. Jackson A, Sheerin K, Reid D, Ganley T, Lamb B, Carroll MR. Custom Foot Orthoses: A Retrospective Analysis of 1000 Prescriptions From New Zealand Podiatrists. J Foot Ankle Res. 2025 Jun 3;18(2).
24. Wang JZ, Wojciechowski EA, Paine T, Burns J, Cheng TL. Feasibility of Designing, Manufacturing and Delivering 3D Printed Ankle-Foot Orthoses: An Updated Systematic Review. J Foot Ankle Res. 2025 Dec 9;18(4).
25. Firoozabadi R, Harnden E, Krieg JC. Immediate weight-bearing after ankle fracture fixation. Adv Orthop. 2015;2015:491976.

Figures

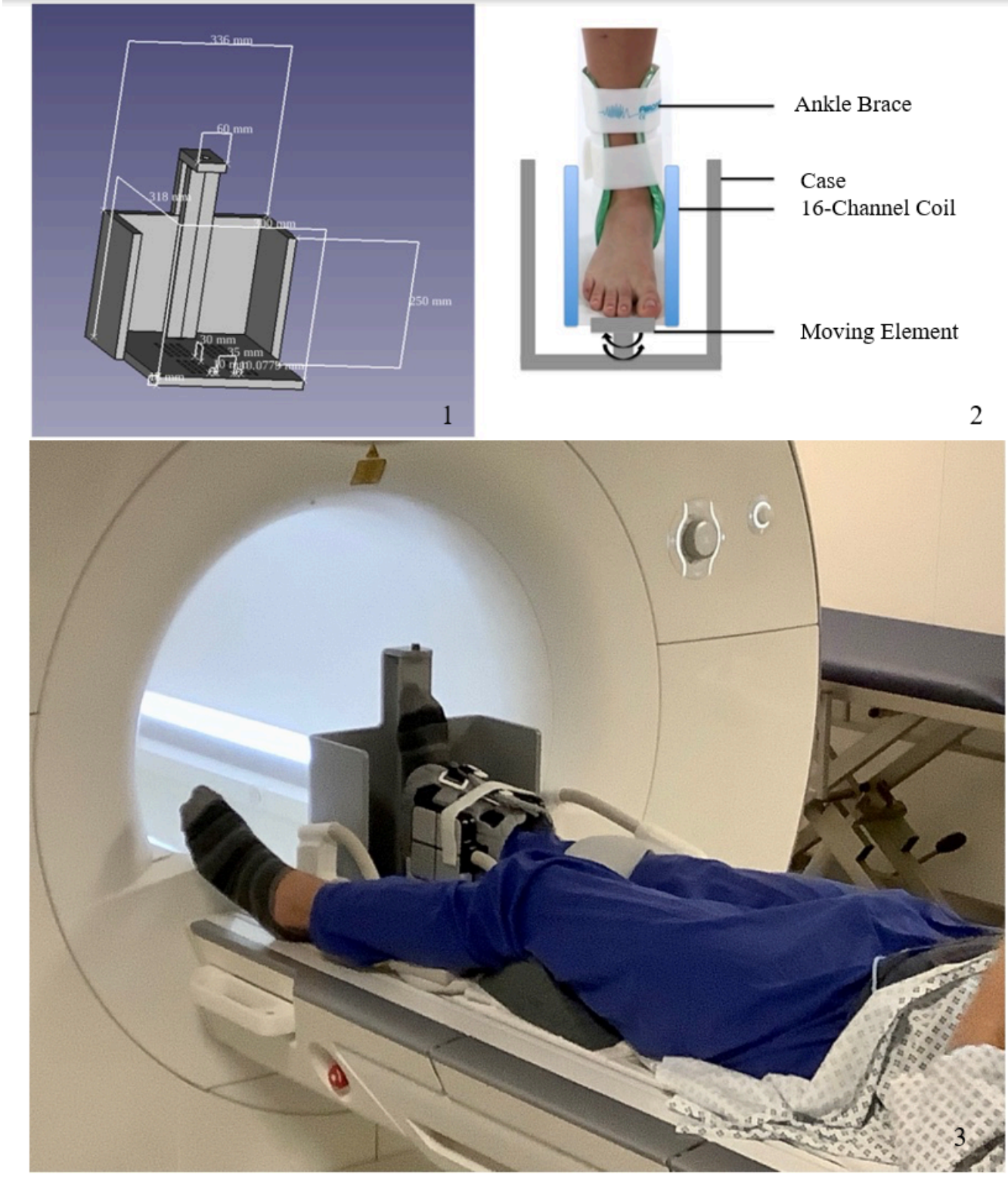


Figure 1

Computer Aided Design (1) and schematic drawing (2) of the specifically designed apparatus for the simulation of eversion and eversion of the ankle joint and MRI setup (3) for measuring the range of motion in inversion and eversion. Written consent was obtained regarding the publication of these images.



Figure 2

Lateral view of the distinct ankle braces used in this study. The models Ottobock 50S8N Malleo TriStep (Ottobock SE & Co. KgaA, Otto Bock Health Care GmbH, Duderstadt, Germany), AIRCAST AIR-STIRRUP II (DJO France, S.A.S., Mouguerre, Frankreich), Push med Ankle Brace (Ofa Bamberg GmbH, Bamberg, Germany) und Juzo Pro Malleo light (Julius Zorn GmbH, Aichach, Germany) were examined. Three of which featured a semi-rigid stirrup design (Ottobock 50S8N Malleo TriStep, AIRCAST AIR-STIRRUP II und Juzo Pro Malleo light). One was a flexible brace (Push med Ankle Brace). Written consent was obtained regarding the publication of these images.

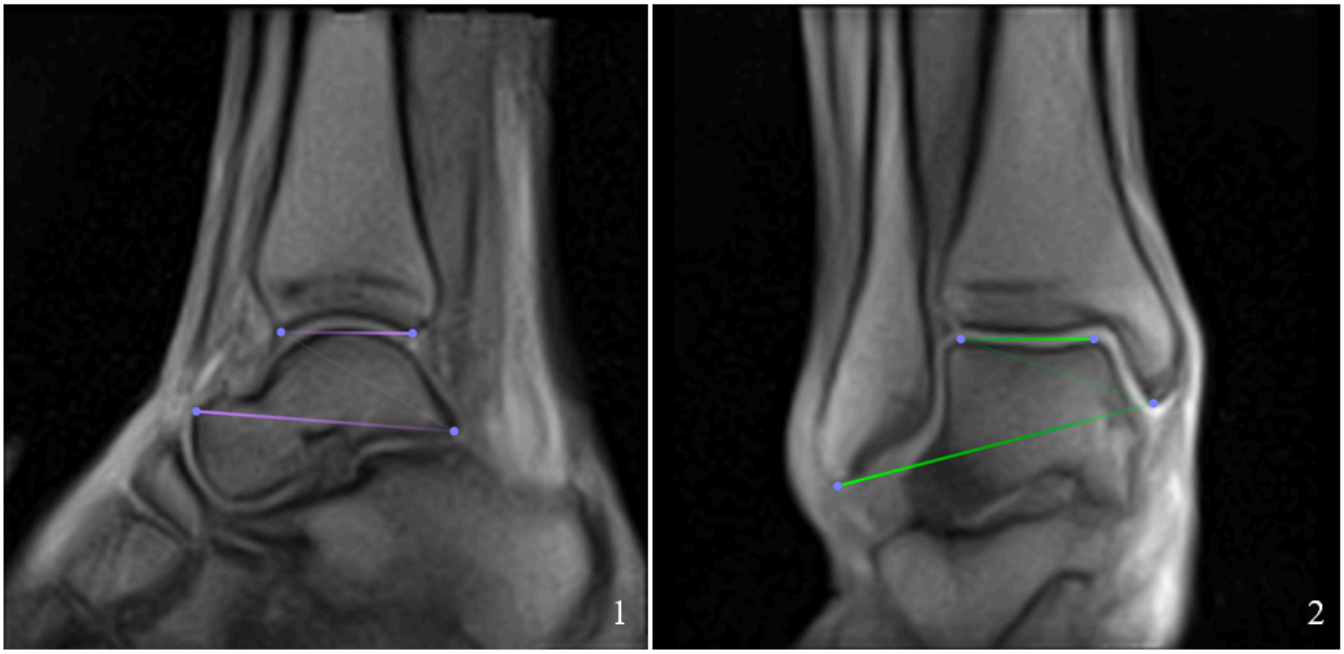


Figure 3

Angle measurements in the sagittal (1) and coronal rtMRI images (2). Written consent was obtained regarding the publication of these images.

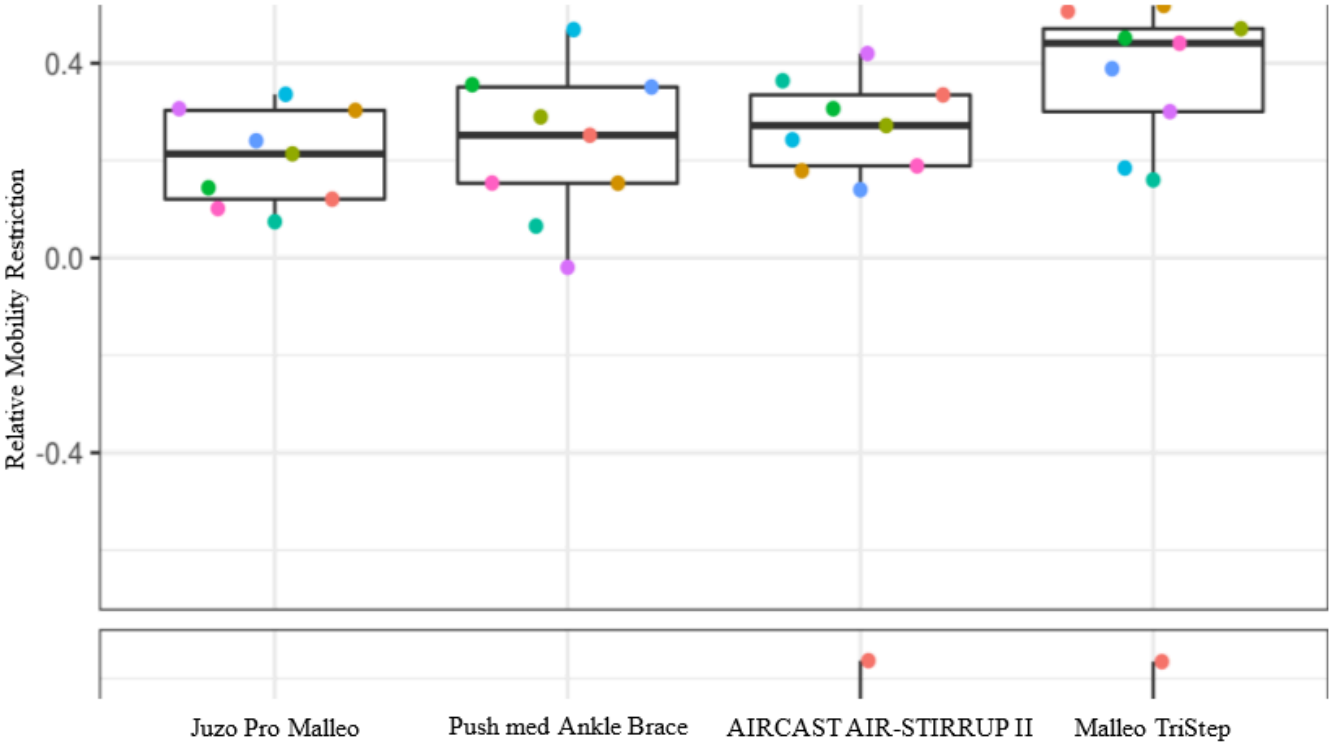


Figure 4

Relative mobility restriction of the different ankle braces in the sagittal plane (plantar flexion/dorsiflexion) compared to the unbraced ankle.

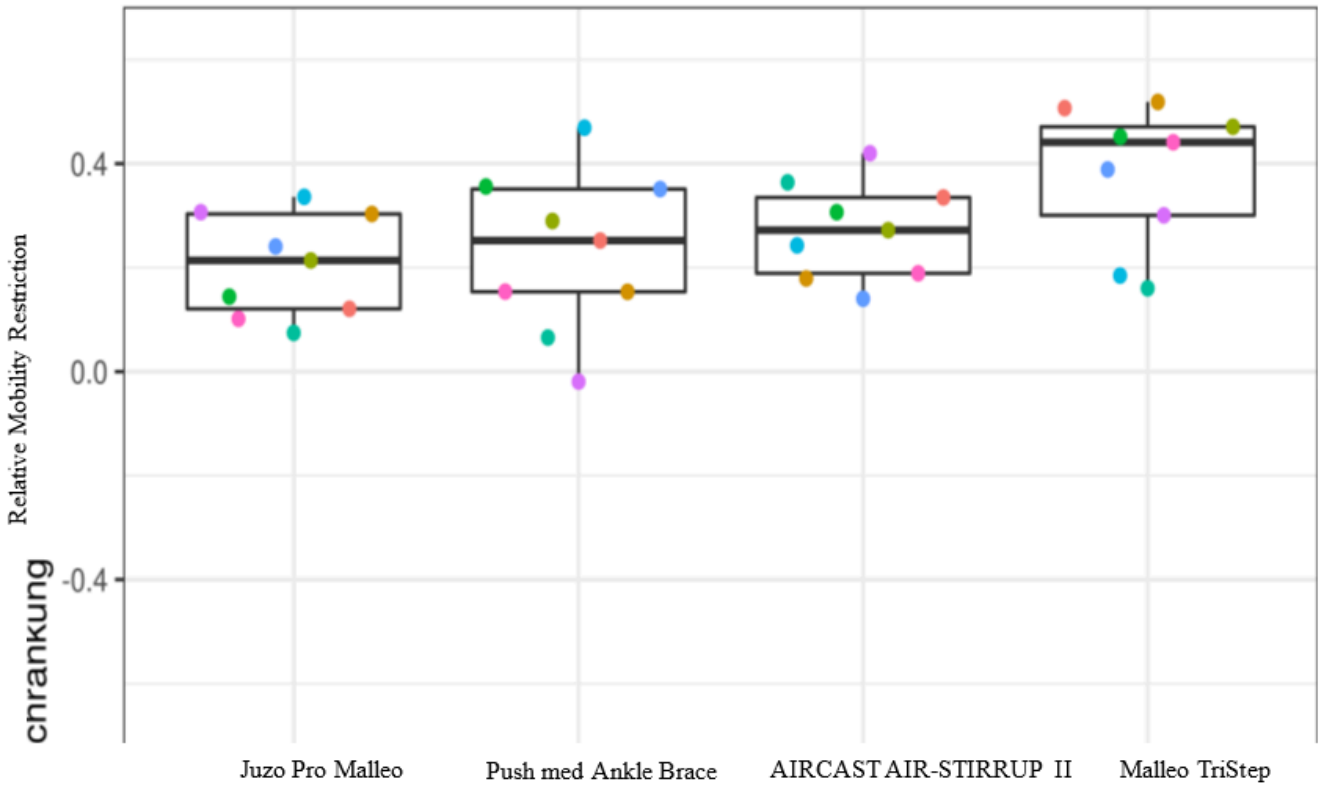


Figure 5

Relative mobility restriction of the different ankle braces in the coronal plane (eversion/inversion) compared to the unbraced ankle.

Supplementary Files

This is a list of supplementary files associated with this preprint. Click to download.

- SupplementalTable1LikertScale.xlsx
- Video1.mp4
- Video2.mp4
- Video3.mp4